ELSEVIER

Journal of Power Sources 67 (1997) 267–278

JOURNAL OF POWER SOURCES

The metallurgy and performance of cast and rolled lead alloys for battery grids

R. David Prengaman *

RSR Technologies, Inc., 2777 Stemmons Freeway, Suite 1800, Dallas, TX 75207, USA

Received 3 October 1996; accepted 26 November 1996

Abstract

This paper evaluates the effects of composition on the mechanical properties of conventionally cast, continuously cast, rolled, and con-cast/rolled lead alloys for battery grids. It outlines the effects of deformation on the mechanical properties of alloys for battery grids, and discuses the influence of alloy composition on corrosion. © 1997 Elsevier Science S.A.

1. Introduction

The lead grid in a lead/acid battery has several functions: it is a collector for current during discharge and charge reactions; it serves to hold the active material; it must corrode to a small amount so that the active material can adhere, but not too much so that the conductive pathways into and out of the battery are lost. The grid must be able to be easily fabricated at high speed, and must not contain deleterious alloying elements or additives that would hinder recycling.

Recent work has indicated that the lead-alloy grid also plays a significant role in determining the ultimate life of the battery. The battery grid must be dimensionally stable and must have sufficient mechanical properties to resist the stresses of the charge/discharge reactions without bending, stretching, or warping. In addition, the battery grid must contain alloying elements (such as antimony or tin) that modify the grid/active-material interface to improve conductivity and resist corrosion that can reduce the cross sections of the grid members. If the battery grid deforms, it can no longer restrain the active material in that dimension. Without restraint, the active material can expand. This expansion causes shedding, loss of capacity and, ultimately, failure of the battery.

Lead–antimony alloys have served as the battery grid alloy for many years. These alloys are extremely strong and creep-resistant and can be cast into rigid, dimensionally stable grids that are capable of resisting the stresses of the charge/discharge reactions. As the antimony content of battery grids has been reduced, the mechanical properties of the alloys has decreased markedly.

Lead–calcium and lead–calcium–tin alloys have increasingly become the alloys of choice for maintenance-free automotive batteries, as well as for valve-regulated lead/acid (VRLA) batteries. In cast form, these alloys are significantly weaker than lead–antimony types. Lead–calcium alloys suffer higher rates of corrosion as the calcium content is increased, but higher calcium contents up to about 0.08 wt.% calcium increase the mechanical properties of the alloys. Tin additions up to 0.7 wt.% have been used to decrease the rate of corrosion and increase the mechanical properties.

Lead–calcium alloy grids have been improved by the addition of even higher amounts of tin as well as silver. These alloys produce higher mechanical properties and greater dimensional stability of battery grids produced by conventional casting as well as from continuously cast strip.

Rolled lead–calcium–tin alloys have demonstrated exceptional mechanical properties. Methods to fabricate grids from the rolled strip by expansion can alter the mechanical properties. The amount of deformation, the alloy, and temperature of deformation all affect the ultimate mechanical properties of the grid. A new continuous-cast rolling process — the Wirtz Con-Roll — can control precisely the initial grid thickness and the amount of deformation for optimum control of mechanical properties, microstructure, and corrosion resistance.

* Corresponding author.

PII S0378-7753(97)02512-3

2. Background

Lead–antimony alloys are used extensively throughout the world as lead/acid battery grids. The antimony content of these alloys varies between 1 and 11 wt.%. Antimony alloys of 4 wt.% and above have traditionally been used for deep-cycling batteries, while alloys with lower antimony content are employed in automotive batteries. Antimony in lead alloys produces high initial mechanical properties, uniform grain structures, and ease in conventional grid casting. On the other hand, lead–antimony alloys are corroded more rapidly than non-antimonial lead alloys when used as battery grids. During cycling, antimony is leached from the positive grid and transferred to the negative. With time, sufficient antimony is deposited on the negative plate to reduce the hydrogen overvoltage and cause the generation of hydrogen gas and, therefore, water loss during cycling.

Low-maintenance batteries have been developed using positives with low-antimony contents (1 to 3 wt.%) and negatives of low antimony or lead–calcium. Traditionally, low-antimony alloys are cast by conventional book-mould procedures and contain nucleants to prevent cracking [1,2]. In recent times, continuous-cast/expanded processes have been developed to produce lead–antimony alloy strip [3] for use in high-speed grid-manufacturing processes. The low-antimony alloys are more difficult to cast and form than high-antimony alloys or other battery alloys because of their large freezing range.

Maintenance-free batteries (whether for automotive, stand-by power, or cycling service) generally use lead–calcium-based alloys. Battery grids have been produced from lead–calcium and lead–calcium–tin alloys via conventionally-cast, continuously cast, continuously cast/expanded strip, as well as continuously-cast/rolled/expanded strip processes. These continuous processes have reduced dramatically the manufacturing costs of batteries and have improved plate uniformity.

Despite the improved processing, positive plates produced from lead–calcium-based grids suffer from active-material shedding, growth, low charge acceptance and reduced cycle life compared with batteries that utilize lead–antimony alloy for the positive-plate grids. The phenomenon of poor cycle life has been called the 'antimony-free effect' and has resulted in premature capacity loss for battery grids produced from lead–calcium alloys.

Recent work by the Advanced Lead–Acid Battery Consortium has indicated that battery construction parameters, particularly compression of the positive active-material, play a major role in the performance of positive plates [4]. The positive battery grid is also important in constraining the active material. Lead–calcium alloys are significantly weaker than lead–antimony alloys, especially with respect to creep resistance [5]. The poor performance of lead–calcium-based positive grids may have been due to improper alloy selection.

It is believed that lead–calcium alloys utilized in cycling and severe service conditions have insufficient mechanical properties, a grain structure conducive to corrosion, and a chemical composition unsuited for optimum performance. Tin additions have been shown to increase mechanical properties, to reduce the tendency towards passivation, to increase corrosion resistance, and to impart stability to grids produced from lead–calcium alloys [6]. Silver also increases both the creep and the corrosion resistance of lead–calcium–tin alloys [7–9].

Working continuously-cast material by rolling (either to produce grids directly or to produce a strip suitable for further processing by expansion) increases the mechanical properties to levels comparable with those of lead–antimony alloys [10]. Understanding the metallurgical aspects of both cast and rolled lead alloys for battery grids has led to improvements in the performance of lead/acid batteries.

3. Lead–antimony alloys

Lead–antimony alloys for lead/acid battery grids have been described by many researchers. The alloys have high mechanical properties due to the presence of a eutectic phase that confers immediate hardness for processing. The alloy also undergoes precipitation strengthening due to antimony as well as other minor alloying elements, particularly arsenic, forming particles within the lattice of the cast alloy. These particles further enhance the mechanical properties.

Because of the high alloy content of most lead–antimony alloys, the grids produced contain a high volume of second-phase particles which inhibit dislocation and grain boundary movement and thus make the grids very stable. Table 1 shows the volume fraction of antimony second-phase particles contained in various lead–antimony alloys. Battery grid alloys also contain alloying elements (e.g., arsenic, copper, sulfur, or selenium). These also produce second-phase particles. Even the low-antimony alloys (1–3 wt.% antimony) contain a significant volume of second-phase particles.

Table 2 lists the mechanical properties as well as the volume fraction of second-phase particles for conventionally-cast plates, continuously-cast strip from the Cominco

Table 1
Volume percentage of second-phase particles in lead–antimony alloys

Antimony content (wt.%)	Volume of particles (%)
11	17.3
6	9.4
4	6.2
3	4.6
2	3.0
1	1.4

Table 2
Mechanical properties and volume fraction of second-phase particles for various alloys

	Antimony content (wt.%)	Volume of second-phase antimony	Total second-phase volume	Yield strength (YS) (MPa)	Ultimate tensile strength (UTS) (MPa)	Ratio YS:UTS (%)	Elongation (%)
Conventionally cast							
	3	4.6	5.0	55.2	65.5	85	10
	2	3.0	3.4	37.9	46.9	80	15
Se	1	1.4	1.8	19.3	32.9	58	20
Continuously cast							
	3	4.6	4.6 (no As)	27.8	35.7	78	15
	1.8	2.7	3.1	26.8	34.0	79	20
Se	1.6	2.4	2.8	25.0	31.8	79	24
Se	1.25	1.8	2.2	23.8	29.6	80	25
Rolled (32:1)							
	3	4.6	4.8	16.3	24.6	66	40

Multi Alloy Caster, as well as rolled strip produced from conventionally-cast material. The conventionally cast material is shown for 1, 2, and 3 wt.% antimony alloys that contain arsenic, copper, and selenium as additional second-phase particles. These increase the volume fraction of particles by about 0.4%.

In conventionally cast grids where solidification is relatively slow, the second-phase eutectic particles are relatively large and a high percentage of the total antimony content can be seen in a grid structure (Fig. 1). These castings also contain a significant amount of second-phase particles that are too small to be detected by light microscopy.

The yield strength is most affected by the small second-phase precipitate particles because they inhibit dislocation and grain boundary movement and decrease permanent deformation of the casting when stresses exceed the yield strength. The conventionally-cast materials have a yield strength that has a high correlation with the amount of second-phase particles in the alloy casting.

As the number of second-paste particles is increased by higher antimony content, the yield strength reaches a higher percentage of the ultimate strength. The higher the yield strength, the greater is the resistance to deformation at a given stress. As the yield stress increases as a percentage of the ultimate tensile strength, the material tends to become more brittle, but less prone to deformation, as shown by the decreased elongation to failure (Table 2). The increased volume fraction of second-phase particles causes a marked increase in the mechanical properties of the conventionally-cast material.

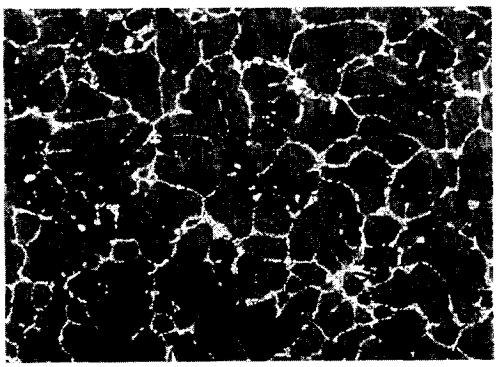

Fig. 1. Grain structure of conventionally cast Pb–3wt.%Sb alloy. (Note: large amount of second-phase antimony eutectic particles; magnification ×320.)

The mechanical properties of continuously-cast strip material also improve, particularly yield strength as a function of increased volume fraction of the second-phase particles. The significant effect of arsenic on mechanical properties in continuously-cast strip [11] is seen in the continuously-cast alloy without arsenic (3 wt.% antimony) which has a much lower yield strength than would be predicted by the volume fraction of particles alone (Table 2).

The continuously-cast material at low-antimony contents has a yield strength that is a higher percentage of the ultimate tensile strength than seen in conventionally-cast materials. Despite this, the material has a higher ductility than conventionally-cast material, the ductility of which declines rapidly with increase in the volume fraction of second-phase particles. The yield strength of the lowest volume fraction material (1.25 wt.% antimony) is proportionally higher than the yield strength of a similar conventionally cast material (1 wt.% antimony), but the ultimate or breaking strength is somewhat lower. This is due to the grain structure and second-phase particle distribution in the continuously-cast material. The continuously-cast material contains significantly fewer visible eutectic particles than conventionally-cast alloys, as seen in Fig. 2. The eutectic has much smaller particles, thus more antimony is present in solution which precipitates as second-phase particles within the lead matrix rather than as large eutectic particles in the grain and sub-grain boundaries. This location of the precipitate is more effective in increasing the yield strength and subsequent creep strength of the material. It should be noted, however, that yield strength is not always relevant to creep working and grid growth in a battery, where the stress is substantially less. If the material is deformed, the directional grain structure causes the movement to be

Fig. 2. Grain structure of Pb–3wt.%Sb alloy cast on Cominco Multi Alloy Caster. (Note: only a small amount of very fine second-phase antimony eutectic particles; magnification ×800.)

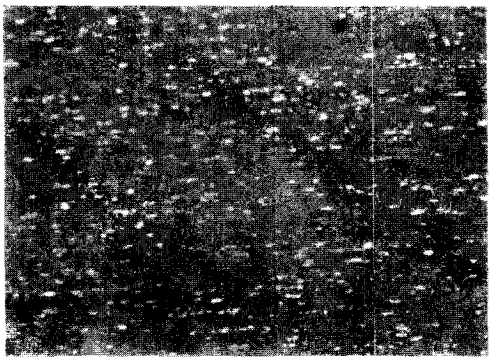

Fig. 4. Grain structure of Pb–3wt.%Sb alloy rolled at a reduction ratio of 32:1. (Note: break-up of coarse antimony eutectic particles and orientation in rolling direction; magnification ×320.)

localized at the grain boundaries. This causes recrystallization and weakening of the material in these localized areas, see Fig. 3u.

The rolled lead–antimony material suffers severe degradation in mechanical properties, despite the presence of a high concentration of second-phase particles as well as the presence of arsenic. The rigid, cast grain-structure is destroyed and the eutectic particles are broken up and elongated in the rolling direction (Fig. 4). The high value of the elongation (40%) is a clear indication that the mere presence of high amounts of second-phase particles alone will not increase the mechanical properties of lead–antimony alloys. The casting creates conditions in the eutectic as well as in the precipitate in the as-cast structure that serve to pin grain boundaries and prevent dislocation movement. These conditions are required for optimum mechanical properties at any loading of second-phase antimony particles. If this structure is disturbed by working (e.g., by rolling or expansion), the precipitate network is broken and results in recrystallization, dissolution of precipitate particles, and lower mechanical properties.

4. Lead–calcium alloys

The mechanical properties of lead–calcium binary alloys are dramatically inferior to those of lead–antimony alloys. The former alloys are used in the negative grids of automotive batteries. The alloys age very rapidly because the strengthening agent, Pb_3Ca, precipitates rapidly from solid solution via a series of cellular precipitation reactions [12,13]. These reactions render the alloys unsuitable for positive-grid alloys because the moving grain boundaries accelerate corrosion and creep under stress.

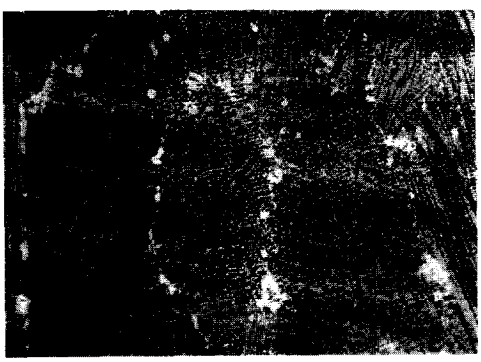

Fig. 3. Grain structure of Pb–3wt.%Sb alloy cast on Cominco Multi Alloy Caster and deformed by stretching. (Note: deformation and recrystallization at grain boundaries; magnification ×320.)

The negative grids of lead/acid batteries can be produced via conventional casting, continuous casting of grids, continuous casting of strip followed by expansion, and continuous-casting/rolling of strip followed by expansion. In all cases, the rapid increase in mechanical properties after casting permits high-speed production and handling of thin (< 1 mm thick) negative plates. The alloys in general use (0.06–0.14 wt.% calcium) have tensile strengths of about 40–45 MPa with excellent ductility for 25–35% expansion. Although the alloys are relatively stable, both the creep resistance and the corrosion rates are inferior to the tin-containing alloys.

Lead–calcium alloys contain a much lower volume of second-phase particles than lead–antimony alloys. The volume percentage of second-phase particles in lead–calcium, as well as in lead–calcium–tin alloys, is given in Table 3. The mechanical properties and rates of ageing for both cast and wrought alloys have been reported [7,13]. In general, rolled alloys have inferior mechanical properties to cast or continuously-cast alloys, but more uniform thickness and ductility.

Table 3
Volume percentage of second-phase particles in lead–calcium and lead–calcium–tin alloys

Calcium content (wt.%)	Volume Pb_3Ca (%)	Volume Sn_3Ca (%)
0.02	0.22	0.25
0.04	0.66	0.75
0.06	1.10	1.26
0.08	1.54	1.77
0.10	1.98	2.29
0.12	2.42	2.73
0.15	3.10	3.39

5. Lead–calcium–tin alloys

Tin additions to lead–calcium alloys increase slightly the volume percent of second-phase particles, as shown in Table 3. $(PbSn)_3Ca$ or Sn_3Ca occupies a slightly larger volume and has higher misfit with the lattice than Pb_3Ca. The increase in the second-phase volume and greater misfit cannot explain fully the much higher mechanical properties attained by lead–calcium–tin alloys. The change in the morphology of the precipitate from Pb_3Ca to $(PbSn)_3Ca$–Sn_3Ca brings about greater stability of the precipitate [14,15].

At any calcium content, increasing the tin content also increases the mechanical properties. The addition of silver slightly increases the mechanical properties while mechanical working by rolling can increase or decrease the mechanical properties, as determined by the ultimate stability of the precipitate.

Table 4 gives the mechanical properties of conventionally-cast samples, continuously-cast plates (thickness: 12.5 mm), continuously-cast strip (thickness: 0.7–0.8 mm) produced on the Cominco Multi Alloy Caster and designed to be expanded into battery grids, and strip rolled from the continuously-cast samples to 1 mm thickness. All samples contain about 0.04 wt.% calcium with various tin contents. All samples were aged for 180 days at room temperature to assure maximum mechanical properties.

There is virtually no difference in the mechanical properties between the thick continuously-cast and conventionally-cast alloys at similar tin contents. The yield strength and ultimate strength increase as the tin content is increased, but the elongation remains virtually the same at about 30%.

The Cominco continuously-cast strip displays lower yield strength and ultimate tensile strength than the conventional-cast or much thicker continuously-cast material. The major difference between the continuously-cast strip and the conventional-cast material is the relatively high yield strength to ultimate tensile strength (YS:UTS) ratio. This phenomenon is similar to that observed with continuously-cast lead–antimony strip. Higher tin additions to the alloy produce higher mechanical properties at room temperature than those obtained by the addition of silver. Even with higher tin contents, however, the mechanical properties of the continuously-cast strip are inferior to those of the same alloys in conventional-cast or thick continuously-cast form.

Rolling the materials increases significantly the mechanical properties of each of the materials. A silver-containing material with slightly higher tin content has been rolled. This material has the highest mechanical properties

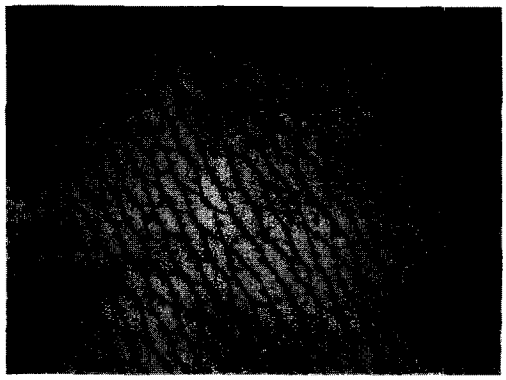

Fig. 5. Typical grain structure for both continuously cast and book-mould cast thick lead–calcium-high tin alloys. (Note: tin segregation to the sub-grains: magnification ×320.)

Table 4
Comparison of mechanical properties of continuously-cast, conventionally-cast, and rolled lead–calcium–tin–(silver) alloys

Ca (wt.%)	Sn (wt.%)	Ag (wt.%)	YS (MPa)	UTS (MPa)	YS:UTS ratio	Elongation (%)
Continuously cast (thickness 12.5 mm) before rolling						
0.044	0.50		38.2	47.8	80	31
0.042	0.73		41.0	50.0	82	28
0.043	1.17		45.6	55.0	83	31
Conventionally cast						
0.048	0.48		38.8	48.6	80	30
0.046	0.70		44.0	53.6	82	30
0.043	1.18		47.1	57.5	82	29
0.045	0.55	0.036	41.6	50.7	82	28
0.042	0.77	0.030	44.2	53.2	83	28
0.046	1.05	0.032	46.0	55.5	83	27
Continuously cast						
0.040	0.95		42.6	47.5	89	30
0.037	0.48	0.034	36.3	40.3	90	24
Concast rolled to 1.1 mm						
0.044	0.50		46.8	57.1	82	17
0.042	0.73		54.6	63.5	86	16
0.042	1.17		57.8	64.3	90	15
0.040	0.62	0.034	64.6	65.4	98	9

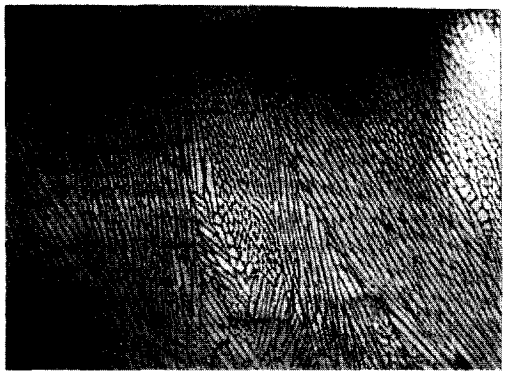

Fig. 6. Typical grain structure for 0.04wt.%Ca–0.9wt.%Sn alloy cast on Cominco Multi Alloy Caster. Large grains grow completely through the concast strip; magnification ×320.

Fig. 8. Complete cross section of 0.04wt.%Ca–0.95wt.%Sn alloy cast on the Cominco Multi Alloy Caster and deformed by stretching. (Note: deformation at grain boundaries and serrated surface; magnification ×320.)

of any of the 0.04 wt.% calcium alloys (Table 4). The yield strength is nearly the same as the ultimate tensile strength. This material should exhibit exceptional creep resistance. As the yield strength is increased (higher tin or silver content), the YS:UTS ratio increases and the elongation decreases.

Typical grain structures of the continuously-cast and conventionally-cast samples are shown in Fig. 5. The grains are large and the sub-grain boundaries become more prominent at higher tin contents. Silver additions at the 0.035 wt.% level exert no effect on the microstructure of these alloys.

The grain structure of the continuously-cast 0.04wt.%Ca–0.95wt.%Sn alloy is shown in Fig. 6. The structure consists of large columnar grains that grow completely through the thickness of the strip. Tin segregation to the sub-grain boundaries is quite clear. When the material is deformed by stretching by about 12%, as would occur in expansion, the large grains slide over one another at the grain boundaries and create a serrated structure at the surface of the strip, see Figs. 7 and 8. There is extensive sliding of the grains over one another to produce areas of fine grains between the large dendritic crystals. As previously reported [16], such a low-calcium, high-tin alloy (without further alloying agents) can suffer severe intergranular cracking and is unsuitable for continuously-cast and expanded grids.

Thin, continuously-cast, strip material that contains silver has a cast structure similar to that shown in Fig. 6 but without tin segregation since the alloy contains significantly less tin. When stretched, the material deforms slightly and creates a serrated surface of the type observed in Fig. 9. On the other hand, the silver content appears to inhibit the severe sliding that occurs in the continuously-cast material without silver.

Rolled material can be worked by bending, slitting or deforming without significant change in the structure of the material. Stretching the rolled material results in stretching of the boundaries and uniform thinning of the material (Fig. 10).

6. Effect of tin on corrosion behaviour of lead–calcium alloys

Tin has been shown [17,18] to exert beneficial properties on the electrochemical behaviour of battery grids. It

Fig. 7. Structure of 0.04wt.%Ca–0.95wt.%Sn continuously cast thin strip deformed by stretching. (Note: the sliding of the grains over one another at grain boundaries; magnification ×320.)

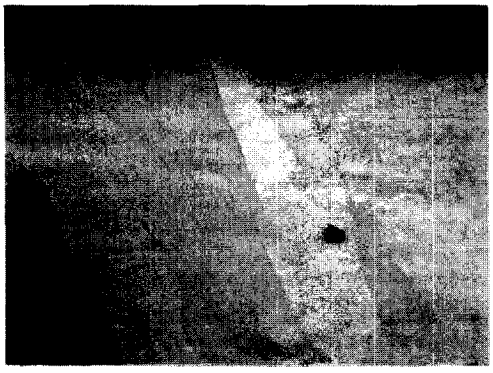

Fig. 9. Grain structure of 0.04wt.%Ca–0.5wt.%Sn–0.3wt.%Ag alloy cast on the Cominco Multi Alloy Caster and deformed by stretching. (Note: only slight sliding of the grain boundaries; magnification ×320.)

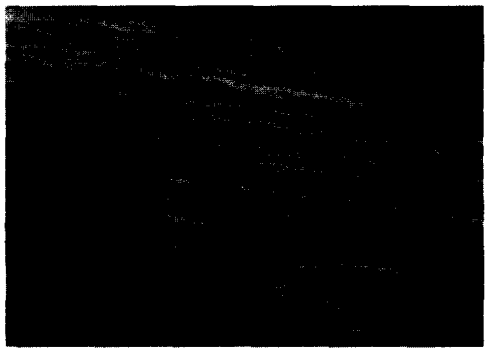

Fig. 10. Grain structure of 0.043wt.%Ca–1.0wt.%Sn alloy rolled to a reduction ratio of 10:1 and subsequently deformed by stretching. (Note: uniform deformation of grain boundaries in the material; magnification ×320.)

helps to resist passivation and to improve recharge performance. Tin has also been shown to improve the corrosion resistance of lead alloys.

The corrosion behaviour of various lead–calcium alloys as a function of tin content is given in Table 5. Samples of lead–calcium and lead–calcium–tin alloys were cast into plates of 6 mm thickness. Samples of these plates were then cut into coupons (70 mm × 19 mm × 6 mm) and weighed prior to testing. The plates were immersed in 1.250 sp. gr. H_2SO_4 with a pure-lead cathode. The plates were anodically corroded at a current density of 0.84 mA cm^{-2} at room temperature (approximately 22 °C) for 1080 h. The samples were then taken from the solution and the PbO_2 corrosion layer removed by treatment with a caustic solution of mannitol and hydrazine dihydrochloride. The samples were washed, dried in alcohol, and weighed to determine weight loss.

Results showed that the corrosion rate increases with calcium content, but decreases with tin content. At a given calcium content, the corrosion rate decreases as the tin content is increased. The corrosion tests were conducted on alloys containing tin up to 1.5 wt.%. Higher tin contents increase the grain size of the alloys, except for the 0.025 wt.% calcium alloys. Thus, the effect of increased tin on the corrosion rate is positive for the last-mentioned alloys.

Table 5
Corrosion behaviour of cast lead–calcium alloys with various amounts of tin

Corrosion rate mils/year at 0.84 mA cm^{-2}						
Ca	Tin content (wt.%)					
(wt.%)	0	0.25	0.5	0.75	1.0	1.5
0.025	11.6	10.2	10.0	10.1	9.7	9.4
0.050	13.6	12.9	12.9	12.0	11.1	10.6
0.065	13.7	13.0	12.7	11.6	10.9	10.8
0.075	14.1	13.1	12.8	11.7	11.7	11.4
0.090	15.4		12.6	12.6	12.3	12.1
0.010	16.2	13.9	13.5	12.7	12.8	11.9
0.012	18.9	14.0	13.8	13.3	13.6	12.8
0.014	20.2	15.5	14.4	14.1	13.8	13.3

Table 6
Effects of deformation ratio and starting billet thickness on the tensile strength of rolled Pb–0.65wt.%Ca–1.3%Sn alloys

Ultimate tensile strength (MPa)						
Deformation	Starting billet thickness (mm)					
ratio	6	12.5	19	25	50	100
2	73.6	71.5	72.2	72.2		
4	71.5	76.4	76.4	75.0	72.9	
8	67.4	72.2	72.2	70.8	71.5	70.1
16	64.6	68.0	68.7	68.0	70.1	68.7
32		66.0	66.6	65.3	64.6	65.3
64			63.1	63.1	62.5	62.8
128					59.7	59.7
256						56.9

7. Effect of amount of deformation on the mechanical properties of lead–calcium–tin alloys

The amount of deformation that a material undergoes during rolling has a significant effect on the final mechanical properties of the rolled strip. Samples of Pb–0.065wt.%Ca–1.3 wt.%Sn alloy were cast at thicknesses of 100, 50, 25, 19, 12.5 and 6 mm. The samples were rolled to reduction ratios of 2, 4, 8, 16, 32, 64, 128 and 256:1 at a deformation of about 25% per pass. The samples were aged for 60 days (fully aged for this alloy) and then evaluated via tensile strength and stress rupture failure (time to failure at 34.6 MPa) as a measure of creep resistance.

The tensile strength of the various materials as a function of deformation ratio is listed in Table 6. The time to fracture as a function of deformation ratio is given in Table 7. Samples of thickness 25 mm and above could not be tested because the thickness exceeded the dimensions of the test equipment. The results show that, in general, there is an increase in mechanical properties with deformation up to a deformation ratio of about 4:1 (i.e., 75% reduction

Table 7
Effects of deformation ratio and starting billet thickness on the stress rupture properties of rolled Pb–0.65wt.%Ca–1.3%Sn alloys

Time to fracture at 34.6 MPa (h)						
Deformation	Starting billet thickness (mm)					
ratio	6	12.5	19	25	50	100
2	14	19	125	38		
4	45	50	407	300	277	
8	5	15	70	44	77	56
16	2	7	50	23	32	44
32		4	8	5	6	5
64			5	2	2	3
128					0.5	1
256						0.5

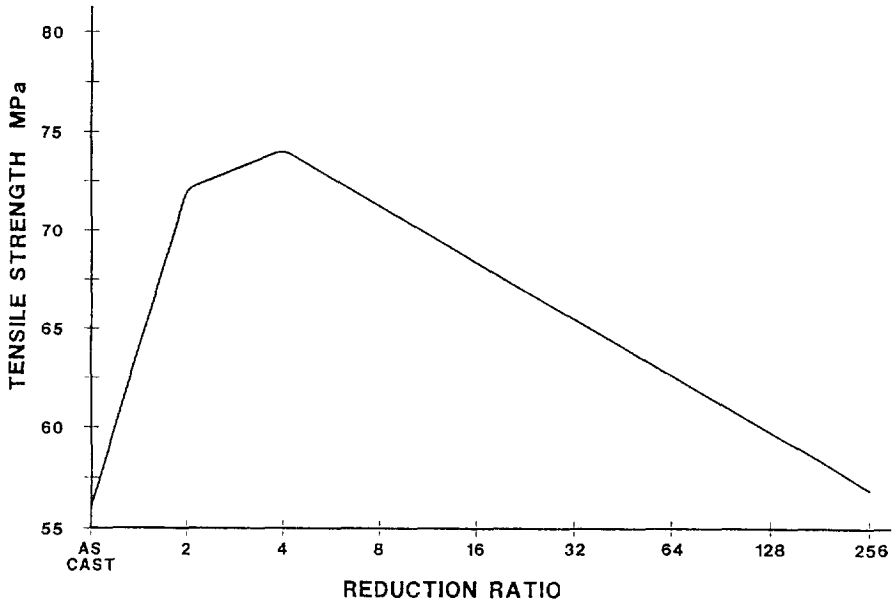

Fig. 11. Effect of reduction ratio on the ultimate tensile strength of fully aged Pb–0.065wt.%Ca–1.3wt.%Sn alloy strip.

in thickness). Beyond such a ratio, the mechanical properties undergo a significant decline in mechanical properties.

The creep resistance suffers an even more rapid decline in properties with deformation. At high deformation ratios, the time to failure is comparable with that of cast alloys. The lead–calcium–tin alloy suffers a decline of over two orders of magnitude as the material is rolled to high reduction ratios. Normal reduction ratios of (10–15):1 yield moderately lower tensile strength, but can reduce the stress rupture resistance at room temperature by a factor of five or more.

The predicted decline in tensile strength and creep resistance as a function deformation ratio is shown in Figs. 11 and 12, respectively. There is a significant drop in the two mechanical properties when the alloy is deformed by more than a 4:1 reduction ratio. At high deformation ratios, the mechanical properties of the material approach those of the cast material.

The effects of deformation ratio can be seen in the microstructure of the rolled alloys. The as-cast microstructure of the 0.065wt.%Ca–1.3wt.%Sn alloy was shown above in Fig. 5. It consists of large columnar grains with interdendritic tin segregation. The microstructure of the same alloy, but now deformed by a reduction ratio of 2:1, is presented in Fig. 13. With this deformation, the original cast grains are bent in the rolling direction and there is significant slip along the interdendritic tin regions. At a

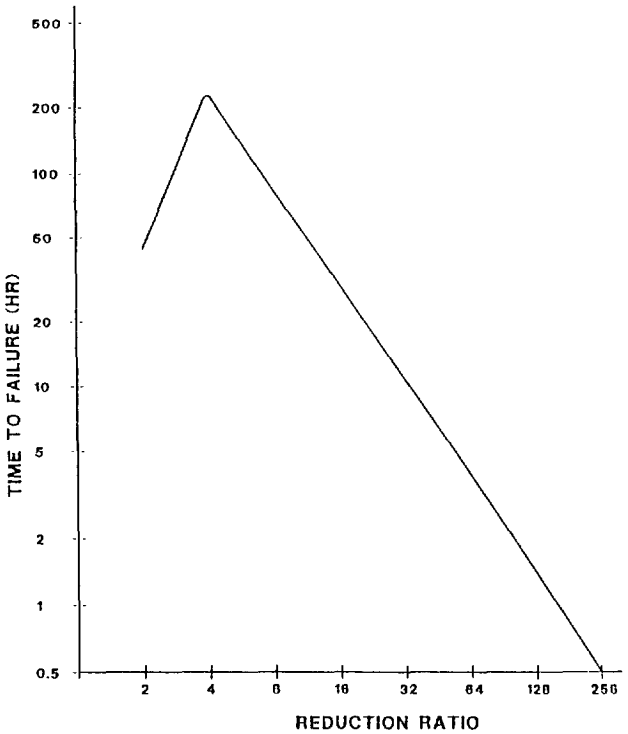

Fig. 12. Effect of reduction ratio on the stress rupture properties of rolled Pb–0.65wt.%Ca–1.3wt.%Sn alloys.

Fig. 13. Initial billet thickness 6 mm rolled to 3 mm, deformation ratio 2:1. (Note: grains turned to the rolling direction; magnification ×320.)

Fig. 14. Initial billet thickness 12 mm rolled to 3 mm, i.e., deformation ratio 4:1. (Note: grains almost completely turned to the rolling direction; magnification ×320.)

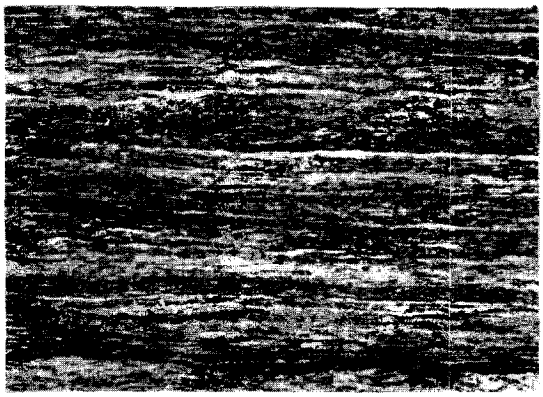

Fig. 17. Initial billet thickness 100 mm rolled to 3 mm, i.e., deformation ratio 33:1. (Note: very fine grains all oriented in rolling direction; magnification ×320.)

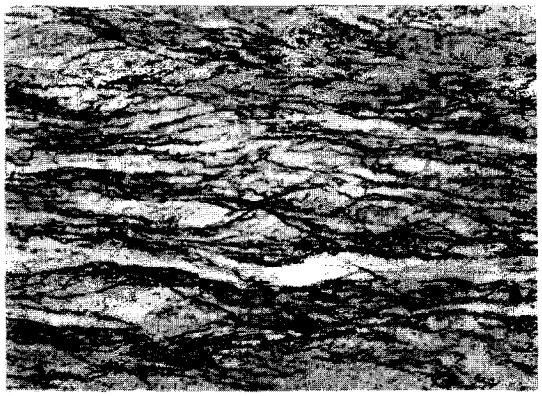

Fig. 15. Initial billet thickness 19 mm rolled to 2 mm, i.e., deformation ratio 6:1. (Note, grains beginning to elongate in rolling direction; magnification ×320._

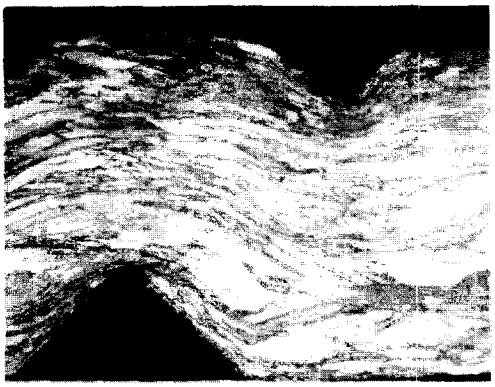

Fig. 18. Grain structure of Pb–0.06wt.%Ca–1.0wt.%Sn alloy battery grid formed by Wirtz Con-Roll process. Material deformed at a reduction ratio of (3–5):1. Deformation caused by knurling to increase paste adhesion; magnification ×320.

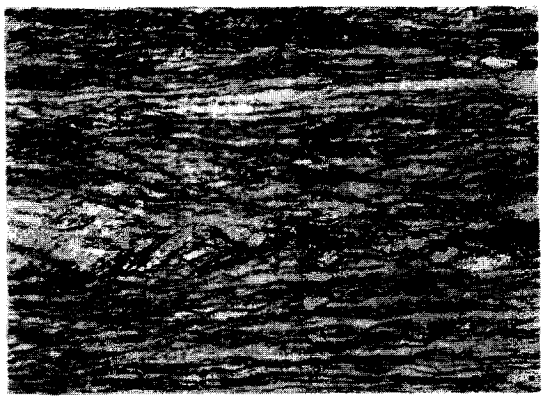

Fig. 16. Initial billet thickness 25 mm rolled to 3 mm, i.e., deformation ratio 8:1. Note, grains beginning to be reduced in thickness; magnification ×320.)

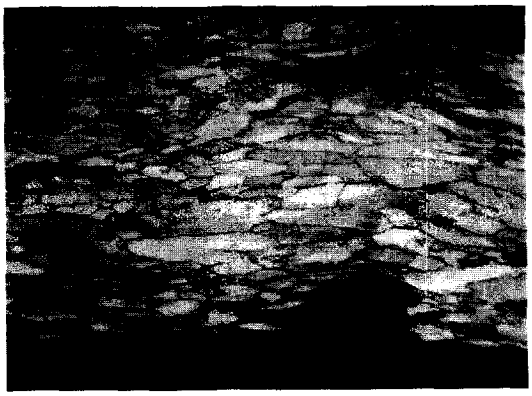

Fig. 19. Grain structure of material in Fig. 18 in transverse direction. (Note: uniform grains; magnification ×320.)

Fig. 20. Grain structure of Wirtz Con Roll Pb–0.06wt.%Ca–1.0wt.%Sn alloy after 2600 hot J240 cycles. (Note: uniform corrosion product and no evidence of corrosion penetration; polarized light; magnification ×320.)

Fig. 21. Grain structure of grid from Fig. 20. (Note: directional grain structure still evident in the grid; magnification ×320.)

reduction of 4:1, the grains are fully bent to the rolling direction (Fig. 14). Beyond a reduction ration of 4:1, the grains become thinned and stretched in the rolling direction (Figs. 15–17). The decrease in mechanical properties can be related to the inability of the precipitated $(PbSn)_3Ca$ particles to strengthen the matrix. This may be due to homogenization of the tin segregation in the alloy.

8. Con-rolled grids

The microstructure of a 0.06wt.%Ca–1.0wt.%Sn alloy that has been continuously cast and rolled into a battery grid by the Wirtz Con-Roll process is shown in Fig. 18. The deformation ratio was about 3.5:1. It can be seen that the original cast grain structure has been turned in the rolling direction and broken down into a wrought structure. The notches in the structure are grooves that are created by knurling the surface for improved paste adhesion. This structure is very stable. The grain structure in the transverse direction is shown in Fig. 19. The grain structure is similar to that produced in the rolling direction. The corrosion profile of the above grid from a battery subjected to 2600 cycles under the hot J240 test is presented in Fig. 20. The material exhibits uniform corrosion with no cracking of the corrosion layer and no attack into the grid. The grain structure of the corroded grid is given in Fig. 21. The original directional rolled structure is maintained; this indicates a stable material. The corrosion product is very similar to that found on conventional wrought-expanded grids (Fig. 22).

9. Stability of rolled lead–calcium–tin alloys

Samples of lead–calcium–tin alloys were rolled at room temperature to a reduction ratio of about 13:1. In an attempt to determine the long-term stability of wrought material, samples were tested to measure ultimate tensile strength during room temperature ageing for up to five years. The results are given in Table 8. The tensile strengths of various alloys are shown after ageing at room temperature for 1, 7, 30 and 60 days, as well as for 1, 3, and 5 years. It was thought that virtually all alloys with an Sn:Ca ratio, R, of 9:1 or more would be stable because the primary precipitate would be the continuous $(PbSn)_3Ca \rightarrow Sn_3Ca$ rather than the discontinuous and unstable Pb_3Ca precipitate. The data reveal, however, that not only should the R value be above 9:1, but the tin content should also be sufficiently high to assure stability in rolled material.

Material with relatively low-calcium and low-tin contents (0.04wt.%Ca–0.25wt.%Sn) declines from the initial rolling strength during ageing ($R = 5.2$). An alloy of 0.044wt.%Ca–0.50wt.%Sn ($R = 11.3$) appears to be stable for up to one year, but suffers a long-term decrease in strength when aged for longer periods. An alloy of 0.042wt.%Ca–0.75wt.%Sn ($R = 17.4$) should be stable, but may not be as stable as it earlier appeared due to a decrease in mechanical properties during long-term ageing.

Once the tin content is increased to over 1 wt.%, the 0.04 wt.% Ca alloys are stable and continue to strengthen with time. At higher calcium contents such as 0.06–0.08

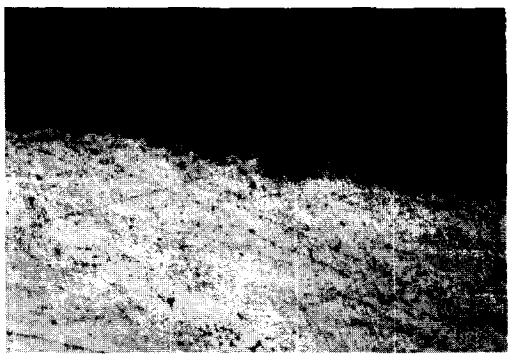

Fig. 22. Grain structure of wrought expanded material from spent battery. (Note: corrosion product on the surface; magnification ×320.)

Table 8
Stability of rolled lead–calcium–tin (UTS, MPa)u

Ca	Sn		Ageing time						
(wt.%)	(wt.%)	*R* value	1 day	7 days	30 days	60 days	1 year	3 years	5 years
0.048	0.25	5.2	35.0	35.4	34.7	34.0	31.9	32.0	32.0
0.044	0.50	11.3	39.0	39.6	43.7	48.0	54.2	40.9	32.0
0.042	0.73	17.4	43.1	44.4	49.3	53.2	61.8	59.7	53.4
0.043	1.17	27.2	44.2	47.9	50.7	62.2	63.8	64.5	65.1
0.049	2.47	50.4	59.2	68.3	72.7	72.3	67.3	50.5	45.3
0.040	0.62	15.5	40.0	41.8	50.3	64.5	65.1	65.1	
	0.034 Ag								
0.069	0.29	4.2	40.9	41.2	41.0	40.0	38.1	37.6	38.1
0.069	0.63	9.1	44.0	48.6	59.0	63.4	61.8	52.7	41.0
0.065	1.00	15.4	47.3	56.9	70.8	70.6	70.8	70.6	70.8
0.061	1.39	22.7	49.2	60.4	70.1	70.8	71.5	71.8	71.5
0.055	1.81	32.9	55.6	66.6	72.9	75.0	74.3	75.0	74.3
0.084	0.51	6.1	47.1	50.7	48.6	47.3	37.5	34.7	34.7
0.085	0.85	10.1	49.3	59.6	68.7	69.6	59.0	53.4	53.4
0.083	1.27	15.3	52.4	65.9	73.6	74.0	75.0	75.0	75.0
0.076	1.80	23.7	54.6	68.0	73.0	72.2	72.2	72.0	72.0

wt.%, the alloys rolled with tin contents above 1 wt.% appear to be stable after even five years of storage. In these alloys, the rolled strip reaches stability after aging for 60 days and remains at that level for the five-year period. Apparently, both the calcium and the tin contents must be sufficiently high to force the precipitation reaction to completion, as well as to produce sufficient second-phase particles for stability.

10. Conclusions

Lead–antimony alloys are extremely strong and stable in the as-cast condition, whether conventionally or continuously cast. Deformation of the cast material by rolling, or the cutting and stretching process of expansion, causes complete or localized break-up of the cast structure, recrystallization, and loss of mechanical properties.

Lead–calcium–tin alloys exhibit increasing mechanical properties and increased resistance to corrosion as the tin content is increased up to about 2 wt.% under both cast and rolled conditions.

For continuously-cast strip produced by the Cominco Multi Alloy Caster, the large directional grain structure and high mechanical properties at high tin and low calcium contents may be detrimental when the material is processed into grids. This is because of non-uniform deformation at grain boundaries. Low tin contents and silver additions to the alloy appear to reduce grain boundary sliding and make the elongation more uniform and less sensitive.

Rolled lead–calcium–tin alloys reach their maximum mechanical properties and creep resistance at a deformation of about 4:1. Further deformation reduces the mechanical properties. At normal rolling reductions of (8–15):1, the rolled material is significantly stronger and more creep resistant than the as-cast material. It is only at extremely high reduction ratios of over 100:1 that the mechanical properties of the rolled material are similar to those of the cast material. The rolled material deforms very uniformly during cutting and stretching into battery grids.

It is believed that lead–calcium–tin alloys with *R* values (Sn:Ca ratios) above 9:1 are stable due to the precipitation of calcium via continuous, rather than discontinuous processes. Wrought lead–calcium–tin alloys with low levels of calcium and tin are found to have decreased properties during long-term ageing despite favourable *R* values. Higher calcium contents produce a higher volume of precipitates. Combined with tin contents of 1 wt.% or more, these alloys provide the required chemical potential to drive the precipitation reactions to completion and thus produce stable materials. Silver additions enhance the stability.

The grids produced by the Wirtz Con-Roll process display high mechanical properties due to a low reduction ratio and a rolled grain structure. The grids are resistant to penetrating corrosion and retain their wrought structure during high-temperature, accelerated life tests of batteries.

Acknowledgements

The author is grateful to Dr E. Valeriote of Cominco, Mr J.O. Wirtz of Wirtz Manufacturing, and Mr M. Boddy of H.J. Enthoven for supplying samples for evaluation. Thanks are also due to Ms I. Betancourt for assistance in the preparation of this paper.

References

[1] R.D. Prengaman, *The Battery Man*, Oct. (1993) 29.
[2] B.E. Kallup and D. Bernot, in K.R. Bullock and D. Pavlov (eds.), *Advances in Lead–Acid Batteries*, The Electrochemical Society, Pennington, NJ, USA, 1984, p. 214.

[3] J. Sklarchuk, M.J. Dewar, E.M. Valeriote and A.M. Vince, *J. Power Sources, 41* (1993) 47.
[4] A.F. Hollenkamp, K.K. Constanti, K.J. Koop and K. McGregor, *J. Power Sources, 55* (1995) 269.
[5] R.D. Prengaman, *J. Power Sources, 33* (1991) 13.
[6] R.D. Prengaman, *Pb–80*, Lead Development Association London, 1980, p. 34.
[7] N.E. Bagshaw, in T. Keily and B.W. Baxter (eds.), *Power Sources 12, Research and Development in Non-Mechanical Electrical Power Sources*, International Power Sources Committee, Leatherhead, UK, 1989, p. 113.
[8] P. Rao, *US Patent No. 5298350* (1994).
[9] L. Albert, *Bright Euram Project BE 7297 Task 8, Progress Rep. ALABC*, Research Triangle Park, NC, USA, 1995.
[10] R.D. Prengaman, *US Patent No. 3953244* (1976).
[11] N.Y. Tang, E.M. Valeriote and J. Sklarchuk, *J. Power Sources, 59* (1996) 63.
[12] H. Borchers, W. Scharfenberger and S. Henkel, *Z. Metallkd, 66* (1975) 111.
[13] L. Bouirden, J.P. Hilger and J. Hertz, *J. Power Sources, 33* (1981) 27.
[14] R.D. Prengaman, *J. Power Sources, 53* (1995) 207.
[15] J. Hertz, C. Fornasieri, J.P. Hilger and M. Notin, *Proc. LABAT '93, Varna, Bulgaria, 1993*, p. 42.
[16] D. Kelly, P. Niessen and E.M.L. Valeriote, *J. Electrochem. Soc., 132* (1985) 2533.
[17] P. Simon, N. Bui and F. Dabosi, *J. Power Sources, 50* (1994) 141.
[18] R.F. Nelson and D.M. Wilson, *J. Power Sources, 33* (1991) 165.